# Spontaneously Organizing Metal Connectors as Supramolecular Structure Directors of Two- and Three-Dimensional Organometallic Assemblies

**Rolf Eckhardt, Hilka Hanika-Heidl, and R. Dieter Fischer*[a]**

**Abstract:** The supramolecular interplay of $Me_3Sn^+$ and $[M(CN)_{2n}]^{n-}$ ions ($n = 3$ and 4) with either 4,4′-bipyridine (bpy), *trans*-bis(4-pyridyl)ethene (bpe) or 4-cyanopyridine (cpy) in the presence of $H_2O$ has been investigated for the first time. Crystal structures of the six novel assemblies: $[(Me_3Sn)_4Mo^{IV}(CN)_8 \cdot 2H_2O \cdot bpy]$ (**8**) and $[(Me_3Sn)_4Mo^{IV}(CN)_8 \cdot 2H_2O \cdot bpe]$ (**8a**; isostructural), $[(Me_3Sn)_3Fe^{III}(CN)_6 \cdot 4H_2O \cdot bpy]$ (**9**), $[(Me_3Sn)_3Co^{III}(CN)_6 \cdot 3H_2O \cdot 3/2\,bpy]$ (**10**), $[(Me_3Sn)_4Fe^{II}(CN)_6 \cdot H_2O \cdot 3/2\,bpy]$ (**11**), and $[(Me_3Sn)_4Ru^{II}(CN)_6 \cdot 2H_2O \cdot 3/2\,cpy]$ (**12**) are presented. $H_2O$ molecules are usually coordinated to tin atoms and involved in *two* significant O–H···N hydrogen bonds, wherein the nitrogen atoms belong either to bpy (bpe, cpy) molecules or to M-coordinated cyanide ligands. Extended supramolecular assemblies such as -CN → $Sn(Me_3)$ ← O(H···)H··N(L)N··HO-(H···) → $Sn(Me_3)$ ← NC- (L = bpy, bpe or cpy) function as efficient metal connectors (or spacers) in the structures of all six compounds. Only in the three-dimensional framework of **11**, one third of all bpy molecules is involved in coordinative N → Sn bonds. The supramolecular architecture of **9** involves virtually non-anchored (to cyanide N atoms), $Me_3Sn^+$ units with a strictly planar $SnC_3$ skeleton, and two zeolitic $H_2O$ molecules. Pyrazine (pyz) is surprisingly reluctant to afford assemblies similar to **8**–**12**, however, the genuine host–guest systems $[(Me_3Sn)_4Mo(CN)_8 \cdot 0.5pyz]$ and $[(Me_3Sn)_4Mo(CN)_8 \cdot pym]$ (pym = pyrimidine) could be isolated and also structurally characterized.

**Keywords:** crystal engineering · hydrogen bonds · structure elucidation · supramolecular chemistry · tin

## Introduction

Organometallic compounds of the type $[(Me_3Sn)_nM(CN)_{2n}] \equiv {}^{q}_{\infty}[M\{\mu\text{-}CNSn(Me_3)NC\}_n]$ ($q = 2$ or 3) with $n = 2$ (M = Ni[1]), 3 (M = Co, **1**[2]) or 4 (M = Mo or W, **2**, **3**[3, 4]) are well-documented coordination polymers, whose metal atoms M may be considered as nodes of four-, six- ,or eight-connected nets. The five-atom metal connectors, or spacers, -CN → Sn ← NC- (type I) usually result by rapid self-assembly when dissolved $[M(CN)_m]^{n-}$ ions meet hydrated $Me_3Sn^+$ ions. The somewhat modified host–guest system $[(Ph_3Sn)_3Fe^{III}(CN)_6 \cdot H_2O \cdot MeCN] \equiv {}^{3}_{\infty}[Fe\{\mu\text{-}CNSn(Ph_3)NC\}_2\{\mu\text{-}CN\cdot\cdot HO(H)Sn(Ph_3)NC\} \cdot MeCN]$ (**4**)[5] is, on the other hand, a heteroleptic congener of **1** and **1a** (M = Fe),[2b] in that its six-connected net contains, in the ratio 2:1, both spacer I and the seven-atom spacer II: -CN··HO(H) → Sn ← NC-. Another long known[6] assembly with a related heteroleptic framework structure is the guest-free system $[(Me_3Sn)_4Fe^{II}(CN)_6 \cdot 2H_2O \cdot diox] \equiv {}^{3}_{\infty}[Fe\{\mu\text{-}CNSn(Me_3)NC\}_2\{\mu\text{-}CNSn(Me_3)O(H)H\cdot\cdot O(diox)O\cdot\cdot HO(H)Sn(Me_3)NC\}]$ (diox = dioxane) (**5**) wherein both spacer I and the notably more expanded spacer III: -CNSnO(H)H··L··HO(H)SnNC- (with L = diox) span a strongly elongated six-connected framework.[7] In view of the spontaneous formation of **4** and **5** from dissolved $R_3Sn^+$ and $[Fe(CN)_6]^{3-}/[Fe(CN)_6]^{4-}$ ions in the presence of acetonitrile and dioxane, respectively, the spacers II and III obviously owe their existence to self-assembly, too.

A possible homologue of **5** containing 4,4′-bipyridine (bpy) instead of dioxane (**6**) is obtained from $[(Me_3Sn)_4Fe(CN)_6]$ (**7**) and bpy in moist acetonitrile as solvent.[8] However, neither single crystals of **6** have so far been obtained, nor could its water content reliably be determined. In principle, the heterocyclic nitrogen base L can either be tin-coordinated, hydrogen-bonded (as diox in **5**) or simply encapsulated by suitable cavities of the guest framework. Herein we focus on the supramolecular architecture of six better crystallizing new, likewise $H_2O$/L-containing compounds with L = either bpy, *trans*-bis(4-pyridyl)ethene (bpe), or 4-cyanoyridine (cpy), **8**/**8a**—**12.**

$[(Me_3Sn)_4Mo^{IV}(CN)_8 \cdot 2H_2O \cdot bpy] \equiv [\mathbf{2} \cdot 2H_2O \cdot bpy]$ **8**

$[(Me_3Sn)_4Mo^{IV}(CN)_8 \cdot 2H_2O \cdot bpe] \equiv [\mathbf{2} \cdot 2H_2O \cdot bpe]$ **8a**

$[(Me_3Sn)_3Fe^{III}(CN)_6 \cdot 4H_2O \cdot bpy] \equiv [\mathbf{1a} \cdot 4H_2O \cdot bpy]$ **9**

[a] Prof. Dr. R. D. Fischer, Dr. R. Eckhardt, Dipl.-Chem. H. Hanika-Heidl
Institut für Anorganische und Angewandte Chemie
Universität Hamburg
Martin-Luther-King-Platz 6, 20146 Hamburg (Germany)
Fax: (+49) 40-42838-2882
E-mail: fischer@chemie.uni-hamburg.de

  0947-6539/03/0908-1795 $ 20.00+.50/0 

$[(Me_3Sn)_3Co^{III}(CN)_6 \cdot 3H_2O \cdot 3/2bpy] \equiv [\mathbf{1} \cdot 3H_2O \cdot 3/2bpy]$ **10**

$[(Me_3Sn)_4Fe^{II}(CN)_6 \cdot H_2O \cdot 3/2bpy] \equiv [\mathbf{7} \cdot H_2O \cdot 3/2bpy]$ **11**

$[(Me_3Sn)_4Ru^{II}(CN)_6 \cdot 2H_2O \cdot 3/2cpy] \equiv [\mathbf{7a} \cdot 2H_2O \cdot 3/2cpy]$ **12**

The presence of bpy, bpe or cpy *together* with $H_2O$ in **8**–**12** suggests that at least part of the bidentate nitrogen base could be hydrogen-bonded to probably metal-coordinated water molecules, affording thus novel, quite extended metal connectors. However, without more detailed structural insights, the possibility of simply encapsulated or Sn-bonded nitrogen bases L cannot strictly be excluded.

## Results and Discussion

### Preparation and general properties of 8-–11

Single crystals of **8**, **8a**, and **10**–**12** suitable for X-ray crystallography were obtained during the long-term exposure of aqueous $K_n[M(CN)_m]$/L solutions to $Me_3SnCl$ vapor, which is in equilibrium with a solid source of this quite volatile compound[1] (route 1). Most unexpectedly, excellent single crystals of **11** were also obtained in low yields during attempts to grow crystals of the coordination polymer $[(Me_3Sn)_6\{Fe^{II}_2(\mu\text{-bpy})(CN)_{10}\}]$[9] from very slowly warmed stacks of initially frozen solutions of $Me_3SnCl$ and $K_6[Fe_2(\mu\text{-bpy})(CN)_{10}]$, respectively, separated by layers of pure ice (route 2). Single crystals of **9** and **10** resulted after one to three days when samples of **1a** or **1** (which are sparingly soluble in pure $H_2O$) had been completely dissolved in mixtures of $H_2O$ (excess), L, and (traces of) MeCN (route 3). While **11** could only be obtained in quantities of up to 10–20 mg, larger polycrystalline (bulk) products of **8, 8a**, **10**, and **12** were readily obtained by co-precipitation. Hereby, an aqueous solution of $K_n[M(CN)_m]$ was added to a solution of $Me_3SnCl$ and L prepared one or two hours before (route 4). Interestingly, addition of $Me_3SnCl$ to $K_n[M(CN)_m]$/bpy solutions led only to markedly bpy-deficient, or even bpy-free, products, suggesting that likewise supramolecular, but still soluble, precursor systems containing hydrated $Me_3Sn^+$ *and* bpy[10] are essential for the successful generation of the new bpy/$H_2O$-containing products.

Surprisingly, experiments carried out according to routes 1 and 4, in which pyrazine (pyz) was used instead of bpy, did not lead to any assembly containing both pyz *and* $H_2O$. Instead, only with $K_4[M(CN)_8]$ (M = Mo, W) as starting components did we obtain genuine host–guest systems such as $[(Me_3Sn)_4Mo(CN)_8 \cdot xL]$ with L = pyz ($x = 0.5$, **13**[11]) and pyrimidine (pym) ($x = 1.0$, **14**[12]) that were structurally characterized. Likewise, single crystals of the guest-free assemblies $[(Me_3Sn)_4M(CN)_8]$ (M = Mo, **15**;[13] M = W, **16**[14]) could be grown by route 1 for the first time. These three products are virtually isostructural with the two earlier reported host–guest systems with L = tetrahydrofuran (thf),[3] although the methyl carbon atoms of **16** turned out to be unusually disordered. While the architecture of the host frameworks remains essentially unchanged, the encapsulated guest molecules (thf,[3] pyz, pym) are always strongly disordered and difficult to identify by X-ray diffractometry alone.

The products **8**, **9**, **10**, and **13** were also subjected to thermal analysis (thermal gravimetry (TG)/differential thermal analysis (DTA), in air). While **8** displayed a continuous weight loss of up to 16.7% between 160 and 260 °C, the genuine host–guest system **13** remained unaffected until 310 °C, whereafter vigorous decomposition took place. Pyrazine was monitored by mass spectrometry (MS) as one of the volatile products. Although the weight loss of **8** corresponded roughly to its total content of $H_2O$ and bpy, fragments of the latter could not be detected by MS, and the powder X-ray diffractogram (XRD) of the solid residue displayed no sharp reflections. Compound **9** starts darkening at 250 °C, although weight loss takes place at $\geq$100 °C (1.13%). Subsequent thermal gravimetic events occurred between 200 and 240 °C (6.95%) and between 240 and 300 °C (37.6%). Reduction of $Fe^{III}$ to $Fe^{II}$ and concomitant liberation of cyanogen are most likely to take place already around 100 °C.

Only the thermal analysis of **10**, along with the identification of the solid residue (obtained at 250 °C) as pure **1**, would justify the assumption of a reversibly regenerable, virtually genuine host–guest system. Decomposition takes place in three steps (90 °C: 4.2%; 140 °C: 19.2%; 260 °C: 28.9%). Although below 250 °C no fragments of bpy were indicated by MS, the IR spectrum of the corresponding solid residue displayed no bands typical of bpy either. However, both the elemental analysis and the XRD of this residue confirmed unambiguously the formation of neat **1**. Moreover, this particular residue could be converted back to **10** (by route 3), and thereafter, again by controlled thermal decomposition, into **1**. According to its elemental analysis, compound **12** seems to lose all its $H_2O$ on drying in vacuo at about 100 °C.

### Crystal structures and vibrational spectra (ν(CN)) of 8—11

**$[(Me_3Sn)_4Mo(CN)_8 \cdot 2H_2O \cdot bpy]$ (8) and $[(Me_3Sn)_4Mo(CN)_8 \cdot 2H_2O \cdot bpe]$ (8a)**: Although the bpe molecule is longer than the bpy molecule (N··N) by about 2 Å, **8** and **8a** turn out to be isostructural.[15, 16] In contrast to the structure of **2**,[3] only four of the eight cyanide ligands of each $\{Mo(CN)_8\}$ fragment are involved in spacers of type I, which leads to the generation of wavy, ABAB-stacked layers (Figure 1). Mo atoms of adjacent layers are connected pairwise by *two* type II spacers, in that $[Mo(\mu\text{-spacer II})_2]_\infty$ strands extend almost perpendicular to the layers (Figure 2). If the bpy or bpe molecules are ignored, the resulting heteroleptic 3D framework can be considered as a six-connected net. Figure 1 offers a view upon two adjacent layers of **8**, and Figure 2 one particular perspective parallel to three adjacent layers. For better clarity, one of the two equivalent layers considered in Figure 1 is presented mainly in black. As in **2**, the coordination geometry of each Mo atom is square antiprismatic.

The bpy molecules actually present in **8**, as well as the bpe molecules of **8a**, are not just encapsulated "mechanically", but distinctly anchored, through two O-H··N hydrogen bonds, to water molecules of type II spacers of two suitably positioned $[Mo\{\mu\text{-spacerII}\}_2]_\infty$ strands (see Figure 2). Overall, the supramolecular assemblies **8** and **8a** may therefore be



0947-6539/03/0908-1796 $ 20.00+.50/0 *Chem. Eur. J.* **2003**, *9*, No. 8

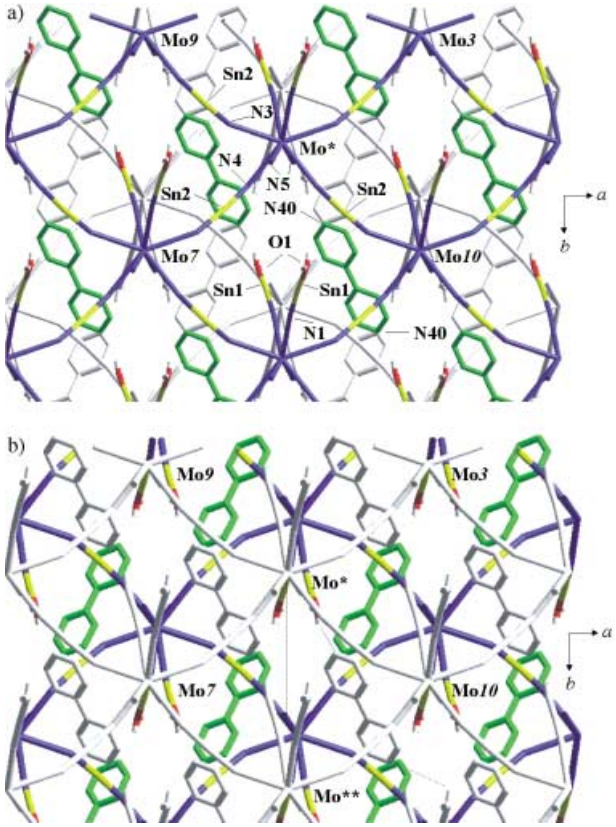


Figure 1. View along the *c* axis upon two subsequent layers (A, B) of **8;** a) in black only layer A and the bpy molecules residing between A and B. b) Alternatively, only layer B and the bpy molecules below it are presented in black. $Mo(CN)_8$ fragments are blue, Sn atoms yellow, O atoms (of $H_2O$) red, and bpy units green; methyl groups have been omitted for clarity. Mo atoms numbered in italics are signified as nearest neighbors of Mo* (see text for details).

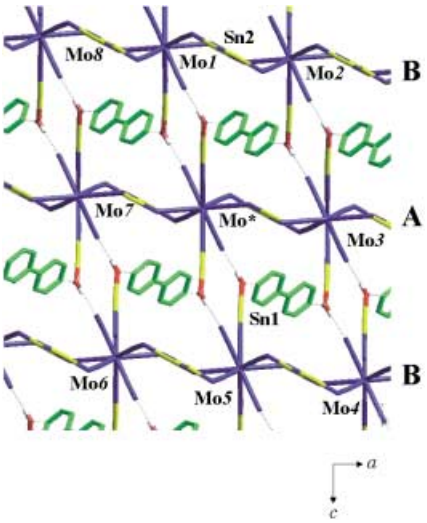


Figure 2. Perspective view of the structure of **8** along three subsequent layers (B, A, B). Methyl groups have been omitted, faint, dotted lines indicate O – H···N hydrogen bonds. Again, Mo atoms numbered in italics are nearest neighbors of Mo* (see text for details).

considered either as heteroleptic, six-connected frameworks with unusually well-fixed guests, or as guest-free systems held together by spacer I and the novel tetradentate spacer (or metal connector) IV (Scheme 1).

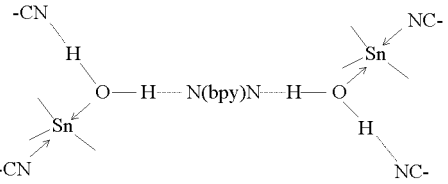


Scheme 1. Tetradentate metal connector of type IV.

In the case of the latter view, **8** and **8a** may formally be understood as ten-connected nets, since then, for example the Mo atom designated by an asterisk in Figure 1 and 2, would not only be connected with the atoms Mo*1*, Mo*3*, Mo*5*, Mo*7*, Mo*9* and Mo*10* (by spacers I or II), but, moreover, (by spacer IV), also with the more distant metal atoms Mo*2*, Mo*4*, Mo*6* and Mo*8*.

Spacer IV clearly comprises not only all of the initially spotted type II spacers, but, inter alia, also the aforementioned spacer of type III with L = bpy. Interestingly, spacer IV is also found in the crystal structures of **9** and **10** (vide infra). For all these assemblies, the O···N(bpy) distances compare well with the O···N(cyanide) distances (see Tables 1 and 2). This feature supports the view that the bpy (or bpe) molecules should be considered as integral parts of distinct metal connectors. Selected structural data of **8** and **8a** are compiled in Table 1. In particular, the seven lowest entries demonstrate that quite a number of distances and angles only undergo rather modest changes to accommodate either bpy or bpe. Although only four of the eight cyanide ligands of each $\{Mo(CN)_8\}$ unit are metal-bridging (Mo-CN → Sn), the IR spectra of both **8** and **8a** display just one sharp and intense ν(CN) band at 2131 $cm^{-1}$ (**2**: 2140 $cm^{-1}$[4]).

**$[(Me_3Sn)_3Fe(CN)_6 \cdot 4H_2O \cdot bpy]$ (9)**[17]: According to a perspective of the structure of **9** viewed along the *a* axis (Figure 3), four of the six cyanide ligands of each $\{Fe(CN)_6\}$ fragment are, as in the structures of **8** and **8a**, primarily

Table 1. Selected interatomic distances [Å] and angles [°] of **8**, **8a**, and **9**.

| **8** | | **8a** | **9** | |
|---|---|---|---|---|
| Sn1–N1 | 2.317(4) | 2.3401(19) | Sn1–N4 | 2.329(3) |
| Sn2–N3 | 2.337(4) | 2.330(2) | Sn2–N2 | 2.651(4) |
| Sn2–N4 | 2.339(5) | 2.336(2) | Sn2–N6 | 2.638(4) |
| Sn1–O1 | 2.288(4) | 2.2487(16) | Sn3–N1 | 2.337(3) |
| | | | Sn1–O1 | 2.202(3) |
| C1-N1-Sn1 | 168.3(4) | 162.47(17) | Sn3–O2 | 2.239(3) |
| C3-N3-Sn2 | 141.3(4) | 145.32(18) | | |
| C4-N4-Sn2 | 148.0(4) | 147.92(19) | C1-N1-Sn3 | 144.9(4) |
| | | | C4-N4-Sn1 | 143.0(3) |
| O1···N5 | 2.777(3) | 2.739(3) | C2-N2-Sn2 | 171.7(9) |
| O1···N40 | 2.760(3) | 2.689(3) | C6-N6-Sn2 | 117.4(13) |
| H1B···N5 | 1.983(3) | 1.90(4) | | |
| H1A···N40 | 2.008(3) | 1.856(10) | O1···N5 | 2.653(4) |
| N5-O1-N40 | 125.2(4) | 117.00(10) | O1···N40 | 2.382(4) |
| Mo*7*···Mo*10*[a] | 16.80(4) | 16.02(4) | O2···N3 | 2.778(6) |
| Mo*···Mo**[a] | 12.46(5) | 13.60(4) | O2···N30 | 2.266(5) |
| Mo*···Mo*1*′[b] | 11.54(5) | 11.70(3) | H1B···N5 | 1.716(4) |
| O1···O1′[c] | 12.62(3) | 14.62(3) | H1A···N40 | 1.769(4) |
| N5-O1-Sn1 | 113.4(3) | 118.94(10) | H2A···N3 | 2.128(6) |
| N5-O1-N40 | 125.2(4) | 117.00(10) | N5-O1-N40 | 120.4(7) |
| N40-O1-Sn1 | 120.9(4) | 116.74(9) | N3-O2-N30 | 113.6(6) |

[a] *Intra*layer. [b] *Inter*layer. [c] With bpy/bpe between O1 and O1′.

  0947-6539/03/0908-1797 $ 20.00+.50/0 

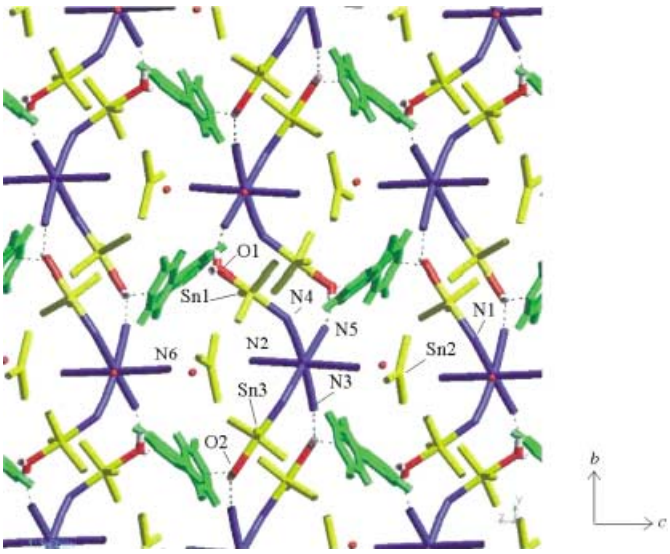


Figure 3. Perspective view of the structure of **9** along the *a* axis. Three $[Mo(\mu\text{-spacerIV})]_\infty$ chains (see the text) extending along the *b* axis are shown. Dotted lines indicate O–H··N(bpy) hydrogen bonds.

involved in the formation of type II spacers, affording again, along the *b* axis, infinite $[Fe\{\mu\text{-spacerII}\}_2]_\infty$ strands with doubly bridged Fe atoms. These strands are interlinked further through very strongly hydrogen-bonded bpy molecules (see Table 1), approximately along the *a* axis, to form infinite, puckered sheets (Figure 4).

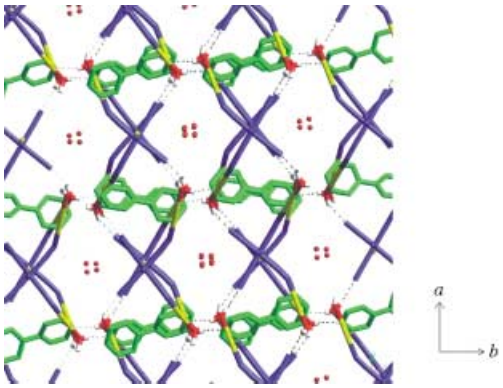


Figure 4. Perspective view of the structure of **9** along the *c* axis. Methyl groups have been omitted for clarity, and dotted lines indicate O–H·· N(bpy) hydrogen bonds.

According to Figure 3, the two *trans*-oriented ligands C(2)N(2) and C(6)N(6) of each Fe atom extending along the *c* axis would appear, in principle, predestinated to generate with the fragment $\{Me_3Sn(2)\}^+$ almost linear, infinite -Fe-CN-Sn-NC- chains. Quite surprisingly, however, the two N–Sn distances of 2.65 and 2.63 Å, found along the *c* axis considerably exceed the usual length of about 2.33 Å typical of spacer I (see Tables 1 and 2), suggesting here unusually weak coordinative interactions. Actually, an Sn–N distance of 2.63 Å would exceed the sum of the covalent radii of Sn and N[18] by about 0.5 Å. Accounting here for the tightly anchored bpy molecules and probably negligible coordinative Sn··N interaction along the *c* axis, the puckered sheets of **9** (vide supra) turn out to be based exclusively on the presence of spacers of type IV as metal-connecting building blocks. In the strict absence of any *coordinative* N→Sn bonding, the cationic $\{Me_3Sn^+\}$ (see also the note added in proof) fragment could be associated with the long-sought stannylium ion.[19] Unfortunately, the paramagnetism of **9** (low-spin $Fe^{III}$ center) does not admit an independent inspection of the effective coordination number of Sn(2) by solid-state $^{119}Sn$ NMR spectroscopy, and an isostructural, diamagnetic homologue of **9** with M = Co has so far not been obtained (vide infra).

In contrast to **8**, **8a**, and **10**–**12**, two of the four $H_2O$ molecules of **9** turn out to be notably disordered, occupying zeolitic positions between the layers. Accordingly, the oxygen atoms O(10) and O(11) give rise to larger thermal ellipsoids than O(1) and O(2) (Figure 5), which are tightly fixed by

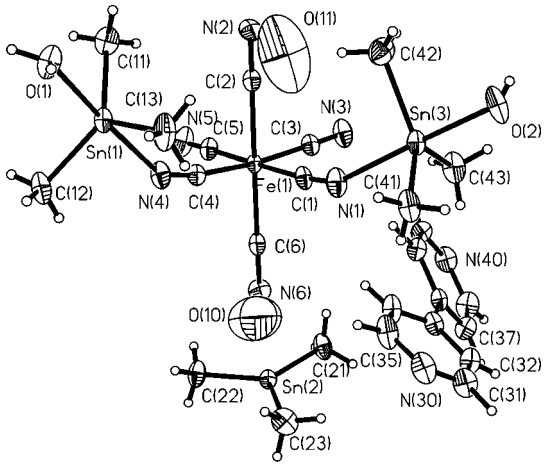


Figure 5. Structure of **9** (asymmetric unit including the atomic numbering scheme; ORTEP plot with thermal ellipsoids represented in 50% probability).

coordinative (O→Sn) and hydrogen bonds. The zeolitic water molecules seem to be well separated from the surprisingly well-encapsulated $Me_3Sn^+$ ions, which otherwise would readily afford $[Me_3Sn(OH_2)_2]^+$ complexes (vide infra). Figure 5 also reveals that the atoms of the potential stannylium ion (as well as N(2) and N(6)) display reasonably small thermal ellipsoids. The two IR-active ν(CN) bands of **9** at 2136 and 2078 $cm^{-1}$ may tentatively be ascribed to CN groups belonging to spacer IV and to the virtually terminal CN ligands (oriented along the *c* axis), respectively.

**$[(Me_3Sn)_3Co(CN)_6\cdot 3H_2O\cdot 3/2bpy]$ (10)**[20]: Quite surprisingly, reaction of **1** (M = Co) and **1a** (M = Fe), respectively, with $H_2O$/bpy (route 3) affords two totally different products. Compound **10** contains, unlike **8** and **9**, bpy molecules in two different structural environments, that is $bpy^A$ and $bpy^B$ (1:2). While $bpy^A$ may again be ascribed to the central component of a tetradentate spacer of type IV, which is responsible for the formation of a negatively charged 3D framework of the net composition $[(Me_3Sn)_2Co(CN)_6\cdot H_2O\cdot 0.5bpy^A]^-$ (vide infra), the $bpy^B$ molecules interlink doubly hydrated $Me_3Sn^+$ ions to infinite, positively charged ribbons (containing $[bpy\cdot H_2O]_\infty$ zigzag chains) of the composition $^\infty_1[Me_3Sn(H_2O)_2\cdot bpy^B]^+_\infty$ (Scheme 2).



0947-6539/03/0908-1798 $ 20.00+.50/0 *Chem. Eur. J.* **2003**, *9*, No. 8

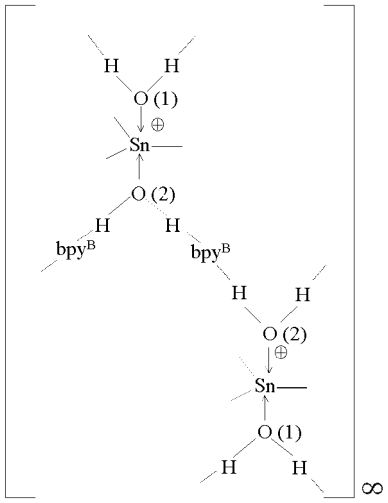


Scheme 2. Infinite, positively charged $[Me_3Sn(H_2O)_2 \cdot bpy^B]^+$ ribbon of **10**.

Basic building blocks of the negatively charged subframework of **10** are parallel zigzag chains involving only spacers of type I. Connectors of type II interlink these chains to puckered, porous layers (Figure 6). Appropriately separated layers are, moreover, connected through two

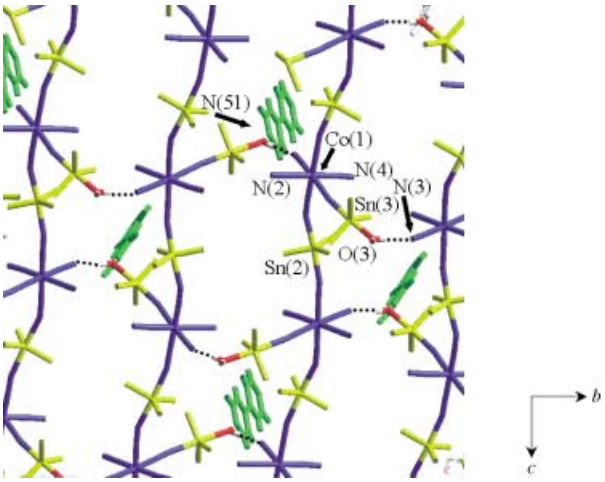


Figure 6. View of one wavy, porous layer constituting the structure of **10** (see text for details). Dotted lines indicate O–H··N hydrogen bonds, and only $bpy^A$ molecules oriented away from the spectator are shown. Color code as in Figure 1

O – H··N($bpy^A$)hydrogen bonds to a voluminous 3D framework (Figure 7). By this latter step, the aforementioned type II connectors are again expanded to tetradentate spacers of type IV. Because of the large internal voids within the resulting negatively charged assembly, two strictly equivalent 3D frameworks undergo mutual interpenetration. This final step parallels the interpenetration of two equivalent, but uncharged 3D frameworks of the earlier reported[7] compound **5** (see the Introduction).

The positively charged ribbons $^{\infty}_{1}[Me_3Sn(H_2O)_2 \cdot bpy^B]^+_{\infty}$ (Scheme 2) extend between two adjacent layers of interpenetrating subframeworks (Figure 8). The tin-coordinated water molecules containing O(1) are then alternantly in-

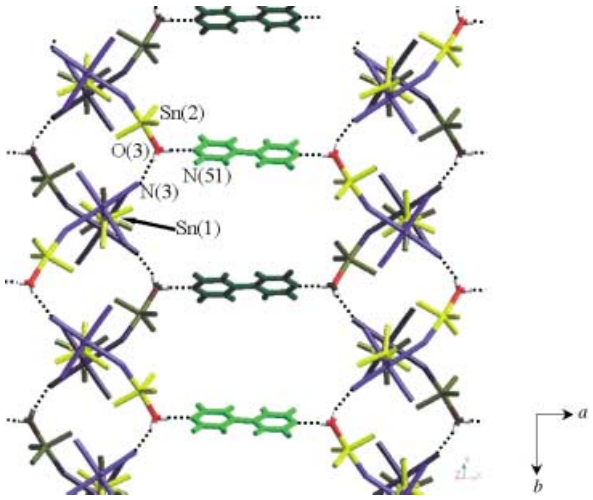


Figure 7. View along two equivalent, porous layers (A, A) of **10** that are connected by $bpy^A$ molecules to an open 3D framework. Light green bpy ligands are located above, and dark green bpy ligands below the projection plane. Dotted lines indicate hydrogen bonds.

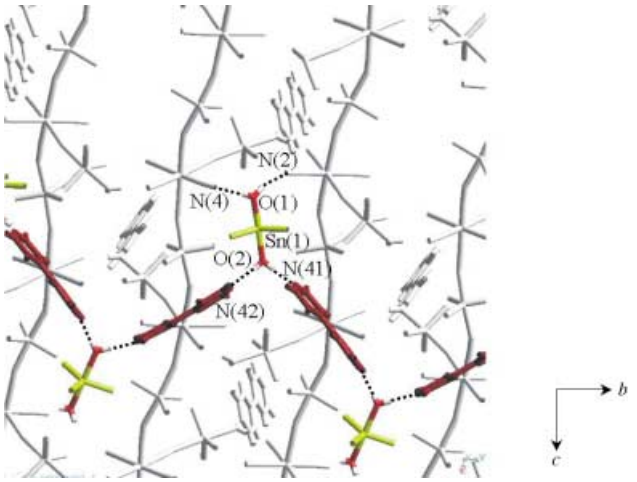


Figure 8. Perspective (as chosen for Figure 6) of the complete structure of **10**. Only the cationic ribbon (see the text and Scheme 2) is comparatively dark. Dotted lines indicate O–H··N hydrogen bonds within the ribbon and with the 3D framework, respectively. Dotted lines indicate hydrogen bonds, and $bpy^B$ molecules are red-brown in color.

volved in O–H··N(cyanide) hydrogen bonds with the otherwise terminal cyanide ligands {C(2)N(2)} and {C(4)N(4)} of either subframework. Owing to this direct involvement of the positively charged ribbon, none of the six cyanide ligands of each $\{Co(CN)_6\}$ fragment will remain strictly terminal. Moreover, by distinct fragments of these chains exceeding in length even spacers of type III (with L = bpy), cobalt atoms of the two interpenetrating subframeworks become also interlinked. Ignoring, however, this latter feature, each cobalt atom of **10** is connected, by spacers of type I and IV, with eight other cobalt atoms. Somewhat surprisingly, **10** gives rise to just one IR-active ν(CN) band (at 2158 $cm^{-1}$), suggesting again that cyanide ligands carrying a tin atom and those involved in CN·· ·H-O(H) → Sn hydrogen bonds, respectively, may have very similar force constants. It is, moreover, noteworthy that all of the $H_2O$ and bpy units of **10** are intrinsic components of a complex supramolecular architecture although, according to

  0947-6539/03/0908-1799 $ 20.00+.50/0 

its thermal behavior (vide supra), **10** behaves like a genuine readily de- and rechargeable, host–guest system.

**[$(Me_3Sn)_4Fe(CN)_6 \cdot H_2O \cdot 3/2bpy$] (11)**[21]: This assembly contains, like **10**, two bipyridine molecules, $bpy^A$ and $bpy^B$ (2:1), in different structural environments, but is devoid of spacers of type IV. Basic building blocks of **11** are quasi-parallel, infinite [Fe-C(1)N(1)-Sn(1)-N(6)C(6)]$_\infty$ zigzag chains (containing only type I spacers) that extend pairwise along the *c* axis. According to a somewhat simplified perspective view along the *a* axis (Figure 9), the Fe atoms of two pairs of chains are connected further by type I spacers (designated as -C(3)N(3)Sn(3)N(4)C(4)-) to infinite ribbons. A characteristic feature of these ribbons is $Fe_3$ triangles with type I spacers as edges.

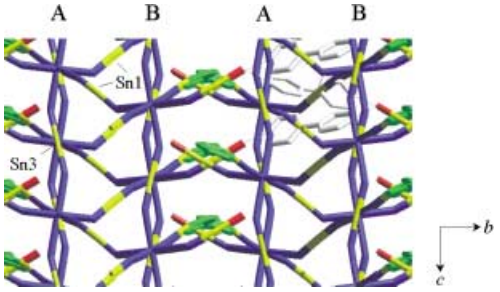


Figure 9. View of four pairs of [Fe-CN-Sn(3)-NC]$_\infty$ zigzag chains (A, B, A, B) of **11**. Adjacent (A,B) ribbons are interlinked by strongly bent CN–Sn(4) ← $bpy^A$ → Sn(4)–NC tethers (type V) with $bpy^A$ molecules (green) almost perpendicular to the projection plane. Only three $bpy^B$ molecules (connecting nonadjacent ribbons) are shown in the upper right segment. Methyl groups have been omitted, and dotted lines indicate O-H · · N($bpy^B$) hydrogen bonds.

Ignoring for a moment the presence of $bpy^B$ molecules (only three of which are drawn in Figure 9), the infinite ribbons turn out to be interlinked by strongly bent spacers of the new type V: -C(5)N(5) → Sn(4) ← N($bpy^A$)N → Sn(4) ← N(5)C(5)-. While Figure 9 suggests, somewhat misleadingly, the presence of infinite sheets, an alternative perspective (along the *c* axis, Figure 10) reveals that even in the absence of $bpy^B$ the framework would not be interrupted along *a*. Actually, infinite *sheets* are stacked along the *c* axis and interlinked by spacers of type I. The tin-coordinated water molecules of **11** (shorter dark lines in Figure 9 and 10) are, finally, involved in the fixation of the $bpy^B$ molecules through strong O-H · · N($bpy^B$) hydrogen bonds (Figure 10 and also Figure 9). As each $H_2O$ ligand makes use of its two hydrogen atoms, infinite zigzag chains as depicted in Scheme 3 result.

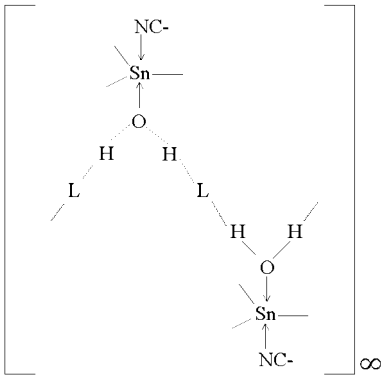


Scheme 3. Infinite [CNSn($Me_3$)($H_2O$) · L]$_\infty$ ribbon of **11** (L = bpy) and **12** (L = cpy).

Scheme 3 differs from Scheme 2 only in that the *peripheral* $H_2O(1)$ ligands present in the latter are replaced by the nitrogen ends of cyanide ligands (coordinated to Fe atoms). Exchange of the two external ($bpy^B$)N · · H-O hydrogen bonds of Scheme 3 by -CN · · H–O bridges would, on the other hand, disrupt the infinite chain into single type IV spacers.

In spacer V the Sn–N(cyanide) distance Sn(4)–N(5) is remarkably short (2.204(5) Å), while the Sn–N($bpy^A$) distance Sn(4)–N(9) is rather long (2.540(5) Å, see Table 2). Sn–N distances involving a {$R_3Sn$} unit and an aromatic nitrogen base frequently exceed 2.5 Å,[19, 22] suggesting only a weak metal-to-nitrogen interaction. Generally, a lengthening of one of the two apical bonds of a trigonal-bipyramidal {A-

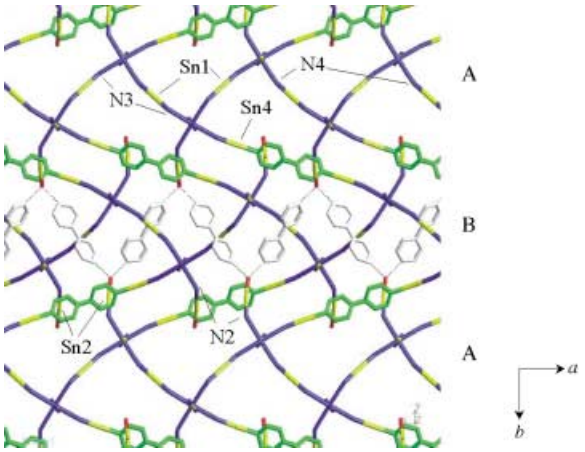


Figure 10. Perspective view of the structure of **11** parallel to three strongly folded sheets (A,B,A). While all $bpy^A$ molecules (green) interlinking adjacent sheets (A,B) are shown, only those $bpy^B$ molecules connecting the two A sheets (only faintly greyish) are displayed. Dotted lines indicate O–H · · N($bpy^B$) hydrogen bonds. All methyl groups have been omitted.

Table 2. Selected interatomic distances [Å] and angles [°] of **10**, **11**, and **12**.

| **10** | | **11** | | **12**[b] | |
|---|---|---|---|---|---|
| Sn2–N1 | 2.350(5) | Sn1–N1 | 2.333(10) | Sn1–N1 | 2.324(3) |
| Sn2–N5 | 2.346(5) | Sn1–N6 | 2.336(9) | Sn1–N14 | 2.296(3) |
| Sn3–N6 | 2.355(5) | Sn2–N2 | 2.242(6) | Sn2–N2 | 2.303(3) |
| Sn1–O1 | 2.276(5) | Sn3–N3 | 2.285(5) | Sn2–N24 | 2.309(3) |
| Sn1–O2 | 2.265(5) | Sn3–N4 | 2.329(5) | Sn3–N3 | 2.303(3) |
| Sn3–O3 | 2.253(5) | Sn4–N5 | 2.209(5) | Sn4–N4 | 2.221(3) |
| | | Sn4–N9[a] | 2.540(5) | Sn3–O1 | 2.447(3) |
| C1-N1-Sn2 | 159.3(5) | Sn2-O1 | 2.117(7) | Sn4-O41 | 2.475(3) |
| C5-N5-Sn2 | 166.3(5) | | | | |
| C6-N6-Sn3 | 157.7(5) | C1-N1-Sn1 | 156.2(5) | O1 · · · N7 | 2.720(4) |
| | | C2-N2-Sn2 | 144.0(6) | O1 · · · N8 | 2.862(5) |
| N2 · · · O1 | 2.699(14) | C3-N3-Sn3 | 162.3(6) | O41 · · · N81 | 2.822(8) |
| N4 · · · O1 | 2.706(17) | C4-N4-Sn3 | 143.0(6) | O41 · · · N82 | 2.917(13) |
| N41 · · · O2 | 2.749(3) | C5-N5-Sn4 | 170.8(6) | | |
| N42 · · · O2 | 2.720(2) | C6-N6-Sn1 | 153.3(5) | O1-H1B-N7 | 102(2) |
| N3 · · · O3 | 2.682(9) | | | O1-H1A-N8 | 161(3) |
| N51 · · · O3 | 2.683(8) | O1 · · · N8 | 2.702(6) | O41-H2A-N81 | 168(3) |
| | | O1 · · · N7 | 2.731(5) | O41-H2A-N82 | 170(4) |
| | | N7-O1-N8 | 95.7(4) | | |

[a] Sn–N(bpy) distance. [b] C-N-Sn angles between 146.1(3) and 164.5(3).



0947-6539/03/0908-1800 $ 20.00+.50/0 *Chem. Eur. J.* **2003**, *9*, No. 8

$Sn(R_3)$-B} system is accompanied by the shortening of the other apical bond (and vice versa). For instance, compounds of the type $[(R_4N)\{(Me_3Sn)_2OH\}Ni(CN)_4]$ display {N-$Sn(Me_3)$-O} fragments with (for R = *n*Bu[23]) rather short O–Sn distances (about 2.15 Å), but unusually long N–Sn distances between 2.529 and 2.546 Å. The almost symmetrical {N··Sn($Me_3$)··N} fragment present in the structure of **9** with *two* even longer N–Sn distances (of ≥2.63 Å, vide supra) contrasts drastically with the usual findings (see also the note added in proof). Another exceptional feature is the less pronounced, but *simultaneous* shortening of both the N(2)–Sn(2) and the O(1)–Sn(2) distances in the {N-$Sn(Me_3)$-O} fragment of **11** (see Table 2).

The three methyl carbon atoms of Sn(4) are bent significantly away from the cyanide nitrogen atom (average C-Sn-N($bpy^A$) angle: 86.5°). The structural findings in total seem to disfavor the view that spacer V involves fragments resembling chemically a $[Me_3Sn(\mu\text{-}bpy^A)SnMe_3]^{2+}$ ion. Such fragments could mimic a hexamethylated, distannamethylviologen cation which might be expected to act as an electron acceptor. Actually, the deep red color of **11**, which contrasts strongly with the practically colorless appearance of **6** and **7**, deserves an explanation. The presence of an electron acceptor close to the powerful electron donor $\{Fe^{II}(CN)_6\}^{4-}$ would admit facile electron transfer. For instance, owing to CT excitation in the visible range, host–guest systems of the type $[(Me_3Sn)_3M^{II}(CN)_6\cdot 0.5MV]$ (M = Fe, Ru, Os; MV = methylviologen dication) are significantly colored.[24] The comparatively broad, IR-active ν(CN) bands of **11** at 2078 sh, 2068, 2053, and 2025 w $cm^{-1}$ seem to reflect the presence of more than three, significantly different CN ligands (actually, there are six nonequivalent ones in the asymmetric unit).

**$[(Me_3Sn)_4Ru(CN)_6\cdot 2H_2O\cdot 3/2cpy]$ (12)**[25]: Basic building blocks of this assembly are strongly folded sheets containing exclusively type I spacers. Figure 11 offers a view upon two subsequent sheets (A and B) which may be distinguished by their shading. Two *cis*-oriented cyanide ligands of each Ru atom carry $Sn(Me_3)OH_2$ units, only one of which is strongly disordered. While two disordered $Sn(Me_3)OH_2$ groups of adjacent sheets (A, B) seem to be connected by one likewise disordered $cpy^A$ molecule, pairs of nondisordered $Sn(Me_3)OH_2$ units from equivalent layers (A,A or B,B) help construct, through well-localized $(cpy^B)N\cdot\cdot H{-}O(Sn\cdot\cdot)-H\cdot\cdot N(cpy^B)$ hydrogen bonds, infinite zigzag chains (see also Scheme 3). A perspective view of the structure of **12** *along* three subsequent layers (ABA) including the disordered and nondisordered bridges, respectively, is given in Figure 12.

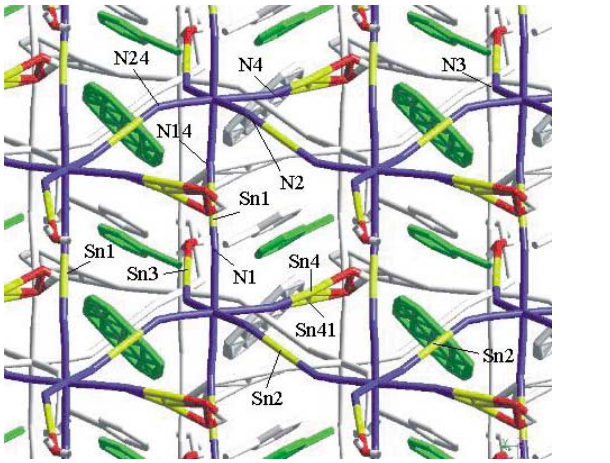


Figure 11. View along *c* upon two adjacent, strongly folded sheets (A, B) of **12**. Only atoms of sheet A are presented in color (for color code see Figure 1). The $cpy^A$ molecules (green) and $Sn(Me_3)OH_2$ fragments (with Sn4 or Sn41) are strongly disordered (see also the two inserts of Figure 12). Methyl groups have been omitted for clarity.

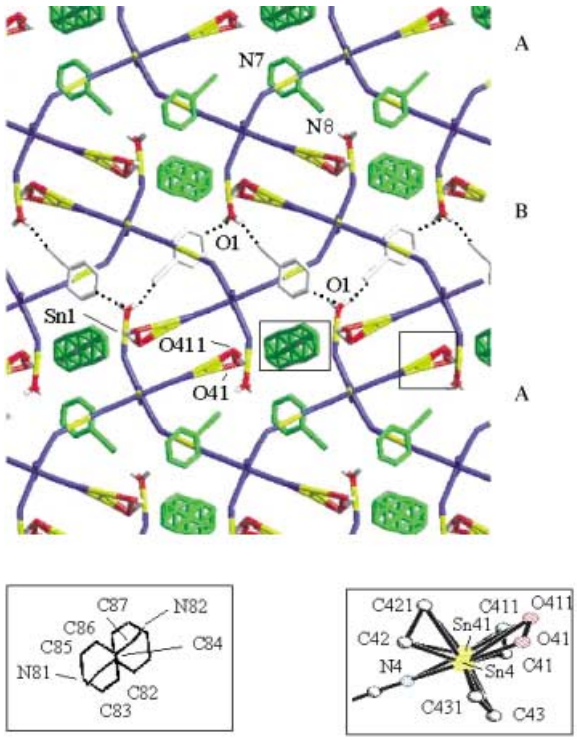


Figure 12. Perspective view of the structure of **12** parallel to three strongly folded sheets (A,B,A). Only the $cpy^B$ molecules connecting the two A sheets have been left uncolored, dotted lines indicate $O{-}H\cdot\cdot N(cpy^B)$ hydrogen bonds. Otherwise, dotted lines and all methyl groups have been omitted. For the disordered $cpy^A$ molecules and $SnMe_3\cdot OH_2$ fragments see the two inserts.

The $cpy^B$ molecules of the infinite zigzag chains are, moreover, oriented in a way that each water molecule forms one hydrogen bond with a nitrile nitrogen atom, and the second hydrogen bond with a pyridyl nitrogen atom. While the $cpy^B$ molecules can again be considered as intrinsic building blocks of quite voluminous three-dimensional frameworks, the $cpy^A$ molecules more likely play the role of less strongly anchored "guests". The supramolecular architecture of **12** may, like the structures of **5** and **10**, again be associated with two equivalent, ideally interpenetrating subframeworks (consisting here either of A or of B sheets only). Interestingly, the perspective view of the sheets A, B, A. of both **11** and **12** as shown in Figure 10 and 12 reveals very similar zigzag chains. Adjacent sheets of **11** (A, B) are interlinked by type V spacers, while equal sheets (A,A; B,B) are connected by type III spacers with L = bpy. Perhaps the significant disorder of the $\{Sn(Me_3)OH_2\cdot cpy^A\}$ fragments of **12** results from the fact that

  0947-6539/03/0908-1801 $ 20.00+.50/0 

spacers of type III with L = cpy[A] would not match in size appropriately with spacer V of **11**. We are only aware of one earlier reported[26] case of an unexpectedly disordered $Me_3Sn$ unit that connects, through CN bridges, two $Cu^I$ ions. Somewhat surprisingly, the IR spectrum of powdered single crystals of **12** did not contain any bands of cpy molecules, although the appearance of the ν(CN) absorption range differs clearly from that of the "precursor" assembly $[(Me_3Sn)_4Ru(CN)_6]$ (**7a**; see Figure 13). In contrast, the IR spectrum of a bulk

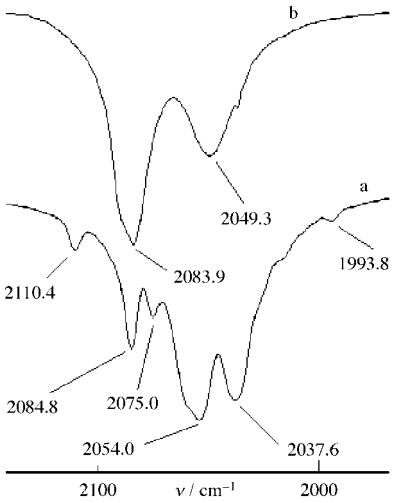


Figure 13. IR bands of **12** (a) and its "precursor" **7a** (b) in the ν(CN) absorption range.

sample of **12** displayed several bands that can be ascribed to cpy (including the nitrile ν(CN) vibration at 2251cm$^{-1}$), whereas here the cyanide ligands give only rise to one rather broad band centered at 2081 cm$^{-1}$. For the final conclusions it should be recalled that the "precursors" of **11** and **12** are, in contrast to, for example, **1** and **2** not strictly homoleptic systems. They are primarily Lewis acidic and not amphoteric like **1**, **1a**, **2**, and **3** (vide infra). Compounds **7** and **7a** are also known to afford derivatives with IR spectra surprisingly rich in ν(CN) bands.[27c]

## Conclusion

While the encapsulation of organic or organometallic cations by negatively charged host frameworks built up of triorganotin(IV) cations and cyanometalate anions has already been described in detail,[24, 26, 27] the corresponding entrapment of uncharged molecules has so far been notably less successful.[28] However, according to the results reported herein, several adducts comprising an uncharged, usually bidentate, nitrogen base L together with two water molecules are readily accessible, owing probably to an efficient synergism of the two cooperating "guests" L and $H_2O$. Whereas most of the hydrophobic, potential host assemblies $[(Me_3Sn)_nM(CN)_m]$ are chemically resistant against neat $H_2O$, the cleavage of a $CN \rightarrow SnR_3$ bond followed by the coordination of a water molecule is strongly stimulated in the presence of a Lewis base L (Scheme 4). Actually, both hydrogen atoms of a tin-

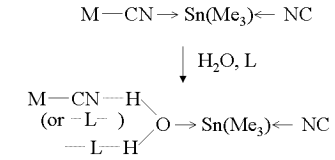


Scheme 4. Essential steps for the remodeling process: homoleptic → heteroleptic assembly.

coordinated water molecule become strongly inclined to form efficient O–H···N hydrogen bonds with L = bpy, bpe, or cpy, and intermediately resulting terminal cyanide ligands, respectively. Bidentate pyridine derivatives tend to build up novel, usually quite extended metal connectors. Interestingly, also with L = acetonitrile,[5] but not with dioxane,[6] both hydrogen atoms of a tin-coordinated water molecule form hydrogen bonds. While the net formulae of **8**–**12**, and several experimentally accessible properties, too, would not rule out a priori the formation of genuine host–guest systems, our single-crystal X-ray studies leave no doubt in the realization of unprecedented, heteroleptic framework structures with a bidentate Lewis base L as the intrinsic component of a supramolecular metal connector. Neither of the structural motifs actually found during our investigation has been predictable. Although, for example, bpy is well known to connect two hydrated metal ions through hydrogen bonds,[29] spacers like those presented in Scheme 1–3 are unprecedented. One of the most exciting results seems to be the lack of type I spacers in the 2D framework structure of **9**, where virtually infinite –[Fe-CN-Sn-CN]- chains appear to be disrupted into isolated $Me_3Sn^+$ ions and nonbridging (terminal) cyanide ligands. It is also noteworthy that, with the exception of compound **11**, the nitrogen base is never coordinated directly to the tin atom, although related compounds involving for example $(bpy)N \rightarrow SnR_3$ bonds have been reported.[18] The O···N(bpy) distances found in **9** are unusually short. In view of the absence of any well-defined type I spacer in **9**, the discovery of other 2D or 3D assemblies involving *exclusively* more extended, supramolecular spacers (than those of type I and type II) does not appear unlikely.[31]

## Experimental Section

**General methods**: Manipulation under an inert gas atmosphere was not necessary. Infrared spectra were obtained on a Perkin-Elmer IR-1720 spectrometer, and TG/DTG studies were carried out on a Netzsch STA 409 instrument equipped with a Balzer QMS 421 quadrupole mass spectrometer. Elemental analyses (C/H/N) were conducted by the elemental analysis service station of the Chemistry Department on instruments of the type Heraeus CHN-O Rapid. X-ray powder diffractograms were obtained at room temperature on a Bruker Advance D8 diffractometer (reflection technique, $Cu_{K\alpha}$ source and Ni filter). Powder X-ray diffractograms (XRDs) were simulated with CERIUS$^2$ 3.0 (MSI), $2\Theta$ range 5–50°. The comparison of experimental and simulated XRDs served as an important method to identify numerous bulk samples.

**Preparation of 8–12**

*Representative description of route 1 (making use of gaseous $Me_3SnCl$) for **8***: Two open, cylindrical 10 mL tubes containing solid $Me_3SnCl$ (0.19 g, 0.98 mmol) and a solution of $K_4[Mo(CN)_8]$ (0.15 g, 0.32 mmol) and 4,4′-bipyridine (0.10 g, 0.64 mmol) in $H_2O$ (ca. 4 mL; plus two drops of acetonitrile) were placed inside a 500 mL flask, which was tightly closed



0947-6539/03/0908-1802 $ 20.00+.50/0 *Chem. Eur. J.* **2003**, *9*, No. 8

and stored at room temperature. Single crystals of **8** optimally suited for X-ray crystallography were harvested after three days, whereas the mainly polycrystalline, yellow bulk of **8** was separated from the mother liquor after one week. Yield (after drying at air): 0.31 g (85 %).

Single crystals of X-ray quality of **8a**, **12**, and **15** could only be obtained when instead of solid $Me_3SnCl$ a relatively concentrated aqueous solution was chosen (ca. 300 mg in 1.5 mL). In this way, the vapor pressure of $Me_3SnCl$ was further reduced, and the crystallization process more favorably slowed down.

*Description of route 2 for **11***: An aqueous solution of $K_6[Fe_2(\mu\text{-bpy})(CN)_{10}]$[30] (0.15 g, 0.20 mmol) in $H_2O$ (10 mL) was frozen under liquid $N_2$, powdered, and placed into a cylindric Dewar container as the lowest layer. Pure, granulated ice (from ca. 30 mL of $H_2O$) was added thereafter as a second layer. The third layer consisted of a likewise frozen solution of $Me_3SnCl$ (0.24 g, 1.20 mmol) in $H_2O$ (5 mL). Optimal thermal isolation permitted thawing periods of 2–4 weeks. Aside various other, unidentified solid products, deep red, needlelike crystals of **11** were finally discovered and manually selected.

*Description of route 3 ("remodeling" of a supramolecular assembly) for **9***: Under stirring, $[(Me_3Sn)_3Fe(CN)_6]$ (**1a**; 0.10 g, 0.14 mmol), was dissolved in a suspension of 4,4′-bipyridine (50.0 mg, 0.32 mmol) in $H_2O$ (50 mL). After 2 h, the filtrate of the almost clear, yellow solution was placed into a closed beaker and stored at room temperature under protection from light. After three days, the continuous growth of reddish-yellow crystals of **9** was finished. Yield: about 0.06 g (45 %).

*Representative description of route 4 (coprecipitation) for **8***: A solution of $Me_3SnCl$ (0.35 g, 1.74 mmol) and 4,4′-bipyridine (0.13 g, 0.86 mmol) in $H_2O$ (50 mL) was, about 2 h after its preparation, united under stirring with a solution of $K_4[Mo(CN)_8]$ (0.29 g, 0.43 mmol) in $H_2O$ (10 mL). The resulting precipitate was washed with small portions of cold water and dried in vacuo. Yield: 0.45 g = 0.39 mmol (91 %).

**8**: Elemental analysis calcd (%) for $C_{30}H_{48}MoN_{10}O_2Sn_4$ (1151.48): C 31.29, H 4.20, N 12.16; found: C 31.28, H 4.40, N 12.16.

**8a**: Elemental analysis calcd (%) for $C_{32}H_{50}MoN_{10}O_2Sn_4$ (1177.52): C 32.64, H 4.28, N 11.89; found: C 32.84, H 4.18, N 11.65.

**9**: Elemental analysis calcd (%) for $C_{25}H_{38}FeN_8O_4Sn_3$ (926.55): C 32.23, H 4.65, N 12.02; found: C 31.56, H 4.23, N 12.02.

**10**: Elemental analysis calcd (%) for $C_{30}H_{45}N_9CoO_3Sn_3$ (994.75): C 36.22, H 4.56, N 12.67; found: C 36.45, H 4.45, N 12.95.

**11**: Elemental analysis calcd (%) for $C_{33}H_{50}FeN_9OSn_4$ (1117.41): C 31.29, H 4.20, N 12.16; found: C 31.56, H 4.23, N 12.02.

**12**: Color yellow; anhydrous sample; elemental analysis calcd (%) for $C_{24}H_{40}N_8RuSn_4$ (1016.50): C 28.35, H 3.97, N 11.02; found: C 28.35, H 3.81, N 10.91.

**13**: Elemental analysis calcd (%) for $C_{24}H_{36}MoN_9Sn_4$ (1006.32): C 26.36, H 3.93, N 12.81; found: C 26.85, H 3093, N 12.57.

**14**: Elemental analysis calcd (%) for $C_{24}H_{40}N_{10}MoSn_4$ (1039.36): C 34.84, H 4.61, N 11.08; found: C 34.60, H 4.38, N 11. 46.

**15**: Elemental analysis calcd (%) for $C_{20}H_{36}MoN_8Sn_4$ (959.27): C 25.04, H 3.78, H 11.68; found: C 25.28, H 3.94, N 11.53.

**16**: Elemental analysis calcd (%) for $C_{20}H_{36}N_8Sn_4W$ (1047.18): C 22.93, H 3.47, N 10.70; found: C 21.30, H 3.24, N 9.81.

**X-ray crystallography**: Data collections were performed at a temperature of 153 K either on a Hilger & Watts Y2900 four-circle diffratometer (**8**, **10**, **11**) or on a Bruker AXS Smart-CCD diffractometer (**8a**, **9**, **12**), (with $Mo_{K\alpha}$ source and graphite monochromator). Individual crystal data are listed in refs. [11–17, 20, 21, 25].

Calculations were based either on the Siemens SHELXTL-93 software or on Bruker SHELXTL programme sets (for Windows), and conducted either on a Micro Vax II computer or on a commercial Pentium III PC (300 MHz). Absorption correction based on symmetry equivalent reflections was automatically carried out by the Bruker instrument applying the SADABS programme. Structures were visualized with the CERIUS² V 4.0 software. $R1 = \Sigma\,||F_o| - |F_c||/\Sigma|F_o|$; $wR2 = \{\Sigma w($
$F_o^2 - F_c^2)^2/\Sigma w(F_o^2)^2\}^{1/2}$.

CCDC-172264 (**8**), CCDC-187720 (**8a**), CCDC-174771 (**9**), CCDC-166200 (**10**), CCDC-174769 (**11**), CCDC-187721 (**12**), CCDC-172267 (**13**), CCDC-172266 (**14**), CCDC-172265 (**15**), and CCDC-172804 (**16**) contain the supplementary crystallographic data for this paper. These data can be obtained free of charge via www.ccdc.can.ac.uk/conts/retrieving.html (or from the Cambridge Crystallographic Center, 12 Union Road, Cambridge CB2 1EZ, UK; Fax: (+44) 1223-336033; or deposit@ccdc.cam.ac.uk).

## Acknowledgement

This work was supported by the Deutsche Forschungsgemeinschaft (DFG), Bonn, within the Priority Programme on Nanostructured Host–Guest Systems. The authors express their deep gratitude to Prof. U. Behrens for valuable crystallographic advice and to S. Samba for diverse technical assistance.

[1] R. Eckhardt, R. D. Fischer, *Inorg. Chem. Commun.* **2000**, *3*, 433–435.
[2] a) K. Yünlü, N. Höck, R. D. Fischer, *Angew. Chem.* **1985**, *97*, 863–864; *Angew. Chem. Int. Ed. Engl.* **1985**, *24*, 879–881; b) U. Behrens, A. K. Brimah, T. M. Soliman, R. D. Fischer, D. C. Apperley, N. A. Davies, R. K. Harris, *Organometallics* **1992**, *11*, 1718–1726.
[3] J. Lu, W. T. A. Harris, A. J. Jacobson, *Angew. Chem.* **1995**, *107*, 2759–2760; *Angew. Chem. Int. Ed. Engl.* **1995**, *34*, 2557–2559.
[4] J.-U. Schütze, R. Eckhardt, R. D. Fischer, D. C. Apperley, N. A. Davies, R. K. Harris, *J. Organomet. Chem.* **1997**, *534*, 187–194.
[5] J. Liu, W. T. A. Harrison, A. J. Jacobson, *Inorg. Chem.* **1996**, *35*, 4271–4273.
[6] M. Adam, A. K. Brimah, R. D. Fischer, X.-F. Li, *Inorg. Chem.* **1990**, *29*, 1595–1597.
[7] R. Eckhardt, Doctoral Dissertation, University of Hamburg (Germany), **2002**, p. 21.
[8] R. Tarhouni, Doctoral Dissertation, University of Hamburg (Germany), **1996**, p. 50.
[9] S. Eller, Doctoral Dissertation, University of Hamburg (Germany), **1992**, p. 69.
[10] For the description of a related, "precursor-like" assembly see: E.-M. Poll, F. Olbrich, R. D. Fischer, *Supramol. Chem.* **2002**, *14*, 309–313.
[11] Crystal structure of $[(Me_3Sn)_4Mo(CN)_8 \cdot 0.5pyz]$ (**13**): $C_{24}H_{36}MoN_9Sn_4$, $M_r = 1006.32$, tetragonal, $I\bar{4}22$, $a = b = 13.0868(3)$, $c = 11.5785(4)$ Å, $V = 1982.98(9)$ Å$^3$, $Z = 2$, $\rho_{calcd} = 1.710$ g cm$^{-3}$, $\mu = 2.152$ mm$^{-1}$, $F(000) = 970$, total number of reflections 27104, unique 1824 ($R_{int} = 0.0559$). Data/restraints/parameters: 1824/0/51, Flack parameter: −0.04(6). Final $R$ indices: $R1 = 0.0315$, $wR2 = 0.0716$ with $I \geq 2\sigma(I)$ and $R1 = 0.0362$, $wR2 = 0.0727$ on all data; goodness-of-fit $S = 1.026$, largest difference peak and hole: 0.897 and −2.587 e Å$^{-3}$.
[12] Crystal structure of $[(Me_3Sn)_4Mo(CN)_8 \cdot pym]$ (**14**): $C_{24}H_{40}MoN_{10}Sn_4$, $M_r = 1039.36$, tetragonal, $I\bar{4}22$, $a = b = 13.0257(4)$, $c = 11.5728(5)$ Å, $V = 1963.54(12)$ Å$^3$, $Z = 2$, $\rho_{calcd} = 1.758$ g cm$^{-3}$, $\mu = 2.846$ mm$^{-1}$, $F(000) = 992$, total number of reflections 14567, unique 1807 ($R_{int} = 0.0461$). Data/restraints/parameters: 1807/0/51, Flack parameter: −0.00(6). Final $R$ indices: $R1 = 0.0326$, $wR2 = 0.0722$ with $I \geq 2\sigma(I)$ and $R1 = 0.0424$, $wR2 = 0.0754$ on all data; goodness-of-fit $S = 0.806$, largest difference peak and hole: 1.248 and −0.910 e Å$^{-3}$.
[13] Crystal structure of $[(Me_3Sn)_4Mo(CN)_8]$ (**15**): $C_{20}H_{36}MoN_8Sn_4$, $M_r = 959.27$, tetragonal, $I\bar{4}22$, $a = b = 12.990(3)$, $c = 11.611(4)$ Å, $V = 1953.31(9)$ Å$^3$, $Z = 2$, $\rho_{calcd} = 1.626$ g cm$^{-3}$, $\mu = 2.843$ mm$^{-1}$, $F(000) = 908$, total number of reflections 48437, unique 1438 ($R_{int} = 0.0477$). Data/restraints/parameters: 1438/6/54, Flack parameter: 0.37(7); final $R$ indices: $R1 = 0.0334$, $wR2 = 0.0840$ with $I \geq 2\sigma(I)$ and $R1 = 0.0370$, $wR2 = 0.0855$ on all data; goodness-of-fit $S = 1.121$, largest difference peak and hole: 1.372 and −0.841 e Å$^{-3}$.
[14] Crystal structure of $[(Me_3Sn)_4W(CN)_8]$ (**16**): $C_{20}H_{36}N_8Sn_4W$, $M_r = 1047.18$, tetragonal, $I\bar{4}22$, $a = b = 12.9748(12)$, $c = 11.3816(16)$ Å, $V = 1916.0(4)$ Å$^3$, $Z = 2$, $\rho_{calcd} = 1.815$ g cm$^{-3}$, $\mu = 5.579$ mm$^{-1}$, $F(000) = 972$, total number of reflections 22745, unique 1442 ($R_{int} = 0.1900$). Data/restraints/parameters: 1442/0/42, Flack parameter: −0.01(2); final $R$ indices: $R1 = 0.0472$, $wR2 = 0.1222$ with $I \geq 2\sigma(I)$ and $R1 = 0.0543$, $wR2 = 0.1301$ on all data; goodness-of-fit $S = 1.215$, largest difference peak and hole: 2.459 and −1.705 e Å$^{-3}$.
[15] Crystal structure of $[(Me_3Sn)_4Mo(CN)_8 \cdot 2H_2O \cdot bpy]$ (**8**): $C_{30}H_{48}MoN_{10}O_2Sn_4$, $M_r = 1151.48$, monoclinic, $C2/c$, $a = 16.797(7)$, $b = 12.464(7)$, $c = 22.240(10)$ Å, $\beta = 108.43(5)^\circ$, $V = 4417(4)$ Å$^3$, $Z = 4$, $\rho_{calcd} =$

1.731 g cm$^{-3}$, $\mu = 2.542$ mm$^{-1}$, $F(000) = 2224$, total number of reflections 5601, unique 4464 ($R_{int} = 0.0302$). Data/restraints/parameters: 4464/0/227. Final $R$ indices: $R1 = 0.0352$, $wR2 = 0.0855$ with $I \geq 2\sigma(I)$ and $R1 = 0.0448$, $wR2 = 0.0904$ on all data; goodness-of-fit $S = 1.023$, largest difference peak and hole: 1.263 and $-1.549$ e Å$^{-3}$.

[16] Crystal structure of $[(Me_3Sn)_4Mo(CN)_8 \cdot 2H_2O \cdot bpe]$ (**8a**): $C_{32}H_{50}MoN_{10}O_2Sn_4$, $M_r = 1177.52$, monoclinic, $C2/c$, $a = 16.023(4)$, $b = 13.603(3)$, $c = 22.572(6)$ Å, $\beta = 110.537(10)^\circ$, $V = 4607(2)$ Å$^3$, $Z = 4$, $\rho_{calcd} = 1.698$ g cm$^{-3}$, $\mu = 2.440$ mm$^{-1}$, $F(000) = 2280$, total number of reflections 34052, unique 8208 ($R_{int} = 0.0387$). Data/restraints/parameters: 8208/6/256. Final $R$ indices: $R1 = 0.0328$, $wR2 = 0.0848$ with $I \geq 2\sigma(I)$ and $R1 = 0.0370$, $wR2 = 0.0862$ on all data; goodness-of-fit $S = 1.058$, largest difference peak and hole: 2.067 and $-1.553$ e Å$^{-3}$.

[17] Crystal structure of $[(Me_3Sn)_3Fe(CN)_6 \cdot 4H_2O \cdot bpy]$ (**9**): $C_{25}H_{38}FeN_8O_4Sn_3$, $M_r = 926.55$, monoclinic, $P2_1/n$, $a = 10.4161(3)$, $b = 19.4120(6)$, $c = 20.6695(7)$ Å, $\beta = 99.4950(10)^\circ$, $V = 4122.1(2)$ Å$^3$, $Z = 4$, $\rho_{calcd} = 1.493$ g cm$^{-3}$, $\mu = 2.175$ mm$^{-1}$, $F(000) = 1808$, total number of reflections 101040, unique 12002 ($R_{int} = 0.0592$). Data/restraints/parameters: 12002/0/435. Final $R$ indices: $R1 = 0.0360$, $wR2 = 0.1053$ with $I \geq 2\sigma(I)$ and $R1 = 0.0498$, $wR2 = 0.1125$ on all data; goodness-of-fit $S = 0.799$, largest difference peak and hole: 1.691 and $-1.697$ e Å$^{-3}$.

[18] See: I. Lange, E. Wieland, P. G. Jones, A. Blaschette, *J. Organomet. Chem.* **1993**, *458*, 57–61, and references therein.

[19] J. B. Lambert, S. Zhang, S. M. Ciro, J. T. B. H. Jastrzebski, *Organometallics* **1994**, *13*, 2430–2443; J. B. Lambert, S. M. Ciro, C. L. Stern, *J. Organomet. Chem.* **1995**, *499*, 49–55.

[20] Crystal structure of $[(Me_3Sn)_3Co(CN)_6 \cdot 3H_2O \cdot 3/2bpy]$ (**10**): $C_{30}H_{45}CoN_9O_3Sn_3$, $M_r = 994.75$, monoclinic, $P2_1/n$, $a = 11.758(11)$, $b = 18.87(2)$, $c = 19.129(12)$ Å, $\beta = 97.86(6)^\circ$, $V = 4206(6)$ Å$^3$, $Z = 4$, $\rho_{calcd} = 1.571$ g cm$^{-3}$, $\mu = 2.186$ mm$^{-1}$, $F(000) = 1956$, total number of reflections 10923, unique 7433 ($R_{int} = 0.0250$). Data/restraints/parameters: 7433/0/496. Final $R$ indices: $R1 = 0.0356$, $wR2 = 0.0841$ with $I \geq 2\sigma(I)$ and $R1 = 0.0588$, $wR2 = 0.0924$ on all data; goodness-of-fit $S = 1.050$, largest difference peak and hole: 0.597 and $-0.674$ e Å$^{-3}$.

[21] Crystal structure of $[(Me_3Sn)_4Fe(CN)_6 \cdot H_2O \cdot 3/2bpy]$ (**11**): $C_{33}H_{50}FeN_9OSn_4$, $M_r = 1117.41$, orthorhombic, $Fdd2$, $a = 28.876(16)$, $b = 59.14(4)$, $c = 10.498(6)$ Å, $V = 17927(20)$ Å$^3$, $Z = 16$, $\rho_{calcd} = 1.656$ g cm$^{-3}$, $\mu = 2.548$ mm$^{-1}$, $F(000) = 8688$, total number of reflections 15508, unique 3861 ($R_{int} = 0.0511$). Data/restraints/parameters: 3861/1/494, Flack parameter: 0.0051. Final $R$ indices: $R1 = 0.0227$, $wR2 = 0.0513$ with $I \geq 2\sigma(I)$ and $R1 = 0.0423$, $wR2 = 0.0558$ on all data; goodness-of-fit $S = 1.058$, largest difference peak and hole: 2.167 and $-2.390$ e Å$^{-3}$.

[22] G. van Koten, *Adv. Organomet. Chem.* **1993**, *35*, 242–246; S. A. Bajue, F. B. Bramwell, M. A. Charles, F. Cervantes-Lee, K. Pannell, *Inorg. Chim. Acta* **1992**, *197*, 83–87; D. Cunningham, T. Higgins, P. McArdle, *J. Chem. Soc. Chem. Commun.* **1984**, 833–835; L. Prasad, Y. LePage, *Acta Crystallogr. Ser. B*, **1982**, *38*, 2890–2893; M. Austin, K. Gebreyes, H. G. Kuivila, K. Swami, J. A. Zubieta, *Organometallics* **1987**, *6*, 834–842; S. Bhandari, C. G. Frost, C. E. Hague, M. F. Mahon, K. C. Molloy, *J. Chem. Soc. Dalton Trans.* **2000**, 663–669.

[23] E. Siebel, R. D. Fischer, J. Kopf, N. A. Davies, D. C. Apperley, R. K. Harris, *Inorg. Chem. Commun.* **1998**, 346–349.

[24] S. Eller, M. Adam, R. D. Fischer, *Angew. Chem.* **1990**, *102*, 1157–1159; *Angew. Chem. Int. Ed. Engl.* **1990**, *29*, 1126–1128.

[25] Crystal structure of $[(Me_3Sn)_4Ru(CN)_6 \cdot 2H_2O \cdot 3/2cpy]$ (**12**): $C_{27}H_{46}N_9RuSn_4$, $M_r = 1104.56$, monoclinic, $P2_1/c$, $a = 10.709(4)$, $b = 15.569(6)$, $c = 25.255(10)$ Å, $\beta = 98.698(10)^\circ$, $V = 4162(3)$ Å$^3$, $Z = 4$, $\rho_{calcd} = 1.763$ g cm$^{-3}$, $\mu = 2.754$ mm$^{-1}$, $F(000) = 2124$, total number of reflections 112294, unique 15082 ($R_{int} = 0.0481$). Data/restraints/parameters: 15082/24/438. Final $R$ indices: $R1 = 0.0373$, $wR2 = 0.0858$ with $I \geq 2\sigma(I)$ and $R1 = 0.0618$, $wR2 = 0.0920$ on all data; goodness-of-fit $S = 1.007$, largest difference peak and hole: 1.694 and $-1.376$ e Å$^{-3}$.

[26] E.-M. Poll, J.-U. Schütze, N. A. Davies, D. C. Apperley, R. K. Harris, *J. Organomet. Chem.* **2001**, *621*, 254–260.

[27] a) A. K. Brimah, E. Siebel, R. D. Fischer, N. A. Davies, D. C. Apperley, R. K. Harris, *J. Organomet. Chem.* **1994**, *475*, 85–94; b) P. Schwarz, E. Siebel, R. D. Fischer, D. C. Apperley, N. A. Davies, R. K. Harris, *Angew. Chem.* **1995**, *107*, 1311–1313; *Angew. Chem. Int. Ed. Engl.* **1995**, *34*, 1197–1199; c) P. Schwarz, S. Eller, E. Siebel, T. M. Soliman, R. D. Fischer, D. C. Apperley, N. A. Davies, R. K. Harris, *Angew. Chem.* **1996**, *108*, 1611–1614; *Angew. Chem. Int. Ed. Engl.* **1996**, *35*, 1525–1527.

[28] See: R. D. Fischer, H. Hanika-Heidl, M. Ling, R. Eckhardt in *Nanoporous Crystals*, (Eds.: F. Laeri, F. Schüth, U. Simon, M. Wark), Wiley-VCH, in press.

[29] See: O. M. Yaghi, H. Li, T. L. Groy, *Inorg. Chem.* **1997**, *36*, 4292—4293, and references therein; see also: S. B. Copp, S. Subramanian, M. Zaworotko, *Angew. Chem.* **1993**, *105*, 755–758; *Angew. Chem. Int. Ed. Engl.* **1993**, *32*, 706–709.

[30] F. Felix, A. Ludi, *Inorg. Chem.* **1978**, *17*, 1782–1784.

[31] Note added in proof (February 19, 2003): According to a new, concerted solid-state NMR and crystallographic study of the 1D polymer $[Me_3SnCN]_\infty$, both interatomic distances along the threefold axis are also unusually long (Sn–Ci 2.295(12) Å; Sn–N: 2.607(11) Å, whereas the NMR shift lies in the usual range as expected for trigonal-bipyramidal configuration. See: P. Avalle, R. R. Harris, H. Hanika-Heidl, R. D. Fischer, *J. Mol. Struct.* **2003**, in press.

Received: July 3, 2002
Revised: September 17, 2002 [F4223]

  0947-6539/03/0908-1804 $ 20.00+.50/0 